Minority carrier diffusion and defects in InGaAsN grown by molecular beam epitaxy

Steven R. Kurtz, J. F. Klem, A. A. Allerman, R. M. Sieg, C. H. Seager, and E. D. Jones

Citation: Applied Physics Letters **80**, 1379 (2002); doi: 10.1063/1.1453480
View online: http://dx.doi.org/10.1063/1.1453480
View Table of Contents: http://scitation.aip.org/content/aip/journal/apl/80/8?ver=pdfcov
Published by the AIP Publishing

Minority carrier diffusion and defects in InGaAsN grown by molecular beam epitaxy

Steven R. Kurtz,[a] J. F. Klem, A. A. Allerman, R. M. Sieg, C. H. Seager, and E. D. Jones
Sandia National Laboratories, Albuquerque, New Mexico 87185-0601

(Received 2 August 2001; accepted for publication 17 December 2001)

To gain insight into the nitrogen-related defects of InGaAsN, nitrogen vibrational mode spectra, Hall mobilities, and minority carrier diffusion lengths are examined for InGaAsN (1.1 eV band gap) grown by molecular beam epitaxy (MBE). Annealing promotes the formation of In–N bonding, and lateral carrier transport is limited by large scale (⩾mean free path) material inhomogeneities. Comparing solar cell quantum efficiencies with our earlier results for devices grown by metalorganic chemical vapor deposition (MOCVD), we find significant electron diffusion in the MBE material (reversed from the hole diffusion in MOCVD material), and minority carrier diffusion in InGaAsN cannot be explained by a ''universal,'' nitrogen-related defect. © *2002 American Institute of Physics.* [DOI: 10.1063/1.1453480]

The quaternary alloy, InGaAsN, is material system with many important potential device applications. Opposite to the trend based on the respective band gaps of GaAs (1.4 eV) and GaN (3.5 eV), addition of a small amount of nitrogen to GaAs radically *lowers* the band gap.[1–3] Addition of indium to GaAsN compensates the strain induced by nitrogen, and with only 3% nitrogen incorporation, one obtains an $In_xGa_{1-x}As_{1-y}N_y$ alloy ($x \approx 0.07, y \approx 0.03$) with a 1.0 eV band gap, lattice matched to GaAs. InGaAsN laser active regions offer the promise of longer wavelength, $\geqslant 1.3$ μm optical transceivers grown on GaAs substrates,[3,4] or record power efficiencies (≈38%) would be obtained with an 1.0 eV, InGaAsN cell added in series to proven InGaP–GaAs tandem solar cells.[5,6] However, for InGaAsN alloys grown by metalorganic chemical vapor deposition (MOCVD) or molecular beam epitaxy (MBE), photoluminescence intensity, and carrier lifetime degrade with increasing nitrogen concentration, and annealing is often required to obtain useful material.[6,7] Observation of complex annealing behavior in both MBE and MOCVD materials suggests the cause is nitrogen-related defects, not atomic impurities. In this work, we examine the defect and transport properties of MBE-grown InGaAsN and compare the properties of the MBE-grown material with those reported for MOCVD-grown InGaAsN. This comparison reveals properties which appear intrinsic to InGaAsN and other characteristics which are unique to a particular growth process. The minority carrier properties of MBE and MOCVD-grown InGaAsN differed, but the diffusion lengths herein still represent the ''state-of-the-art,'' with only mediocre solar cell performance obtained with either growth process.

$In_{0.07}Ga_{0.93}As_{0.98}N_{0.02}$ (1.1 eV band gap) was grown by MBE at a temperature of ~430 °C. Nitrogen was supplied by a radio-frequency plasma source, while the remainder of the constituent elements were evaporated from conventional solid sources. *Ex situ*, postgrowth annealing of this material at 900 °C for 10 s improved the photoluminescence efficiency and subsequent device performance. The band gap, observed through photoluminescence or absorption, increased ~20 meV due to incremental nitrogen loss during annealing. A band-gap photoluminescence peak [≈40 meV (FWHM) @ 300 K] was observed in unintentionally doped, *p*-type (mid-10^{16}/cm^3) material. Peak intensity increased ≈10× upon annealing the undoped material. For Si doped, *n*-type material, photoluminescence spectra exhibited a very broad peak encompassing the band gap at the highest energies. Overall, photoluminescence of the MBE material displayed characteristics similar to those we have observed for MOCVD samples.[6]

Looking for a mechanism to explain annealing behavior, we examined nitrogen-related local-vibration-modes (LVMs). Fourier transform infrared transmission spectra are shown for an annealed and as-grown, undoped InGaAsN (1.1 eV) sample in Fig. 1. Prior to annealing, a single LVM line is observed at 468 cm^{-1} which corresponds to the Ga–N mode at 470 cm^{-1} reported for GaAs:N.[8] No evidence for In–N bonds was observed prior to annealing.[9,10] Annealing produced In–N bonds, and three LVMs were observed at 457, 489, and 515 cm^{-1}. With the larger mass of the indium atom, the line at 457 cm^{-1} corresponds to an In–N stretch, and the Ga–N stretch is shifted to 489 cm^{-1} in a Ga_3InN cluster.[9] Similar behavior was reported by S. Kurtz *et al.* in MOCVD-grown (~550 °C) InGaAsN samples with lower nitrogen content (0.2%).[9] They still observed a Ga–N, 470 cm^{-1}, peak after annealing at 700 °C for 30 min, whereas in our MBE samples that peak disappeared after annealing which indicates that almost 100% of the nitrogen atoms formed In–N bonds. In–N pairing minimizes strain energy in the GaAs-like lattice. We speculate that the 515 cm^{-1} line may be associated with Ga_2In_2N clusters. Our infrared studies of MOCVD-grown InGaAsN (2% N, 600 °C growth) were inconclusive due to broadened and distorted (''Fano'') LVM line shapes.

We examined the effect of these annealing-induced structural changes on Hall transport. Of particular interest, strong random alloy fluctuations in InGaAsN may result in electron localization.[11] Hall mobility and carrier concentra-

[a]Electronic mail: srKurtz@sandia.gov

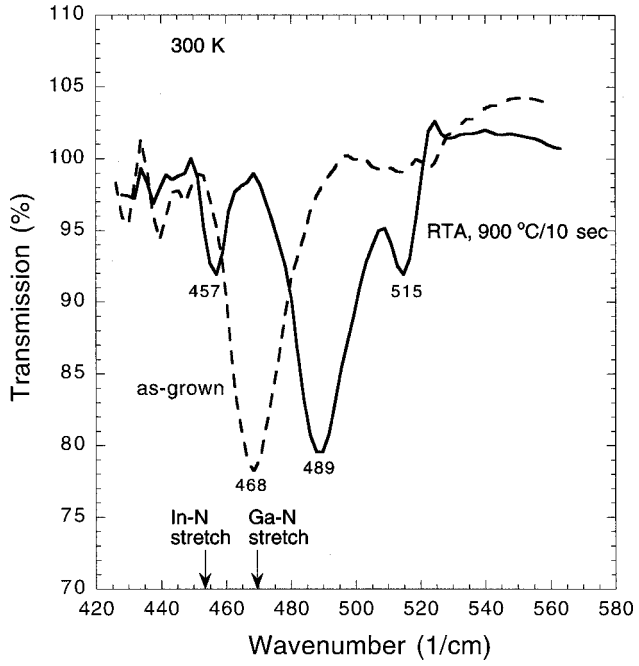

FIG. 1. Infrared transmission spectra for a MBE grown, 0.6 μm thick $In_{0.07}Ga_{0.93}As_{0.98}N_{0.02}$ sample as-grown (dashed) and *ex situ* annealed (solid) at 900 °C for 10 s.

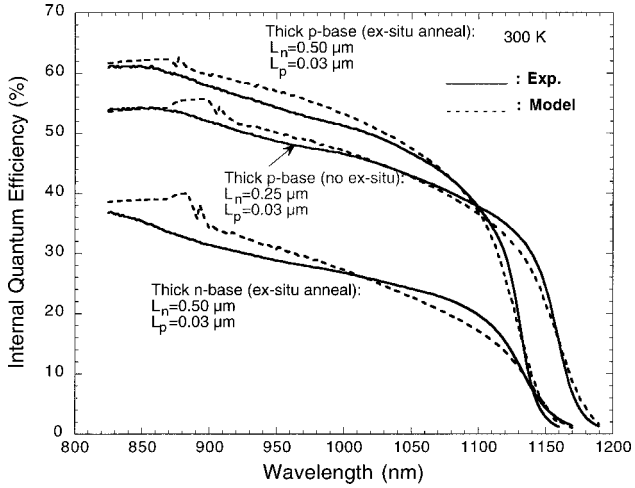

FIG. 3. Spectral response of three MBE-grown InGaAsN solar cells, thick *p*-base (*n*-on-*p*, with and without *ex situ* anneal) and thick *n*-base (*p*-on-*n*, *ex situ* annealed) devices. Cell simulations (dashed lines) and respective electron (L_n) and hole (L_p) minority carrier diffusion lengths are indicated for each cell.

tion temperature dependencies are shown in Fig. 2 for *n*-type MBE-grown InGaAsN (1.1 eV). After annealing, the electron concentration (high-10^{16}/cm^3) was weakly temperature dependent, and the mobility changed by only 3× over 300–16 K. These Hall data for the annealed MBE InGaAsN were very close to those reported for annealed MOCVD material with nominally the same composition and doping level. As before, we attribute the mobility temperature dependence to large scale (≫mean free path) inhomogeneities or potential barriers.[11] The highest mobility for the MBE material was ≈300 cm^2/V s, consistent with the limit imposed by alloy scattering at this nitrogen concentration.[12] In the unannealed, as-grown MBE sample, we observed strong thermal activation of both mobility and carrier concentration. An activated carrier concentration suggests a trap-modulated mobility with a mobility edge. An activated carrier concentration was not observed in unannealed InGaAsN grown by MOCVD at 600 °C, and we associate the localization in as-grown MBE InGaAsN with structural disorder resulting from the lower temperature MBE growth. Annealing also produced a 5× increase in the conductivity of *p*-type InGaAsN grown by MBE.[13] Perhaps defects inferred from LVM spectra or excess nitrogen[14] produce localization observed in InGaAsN grown at lower temperature.

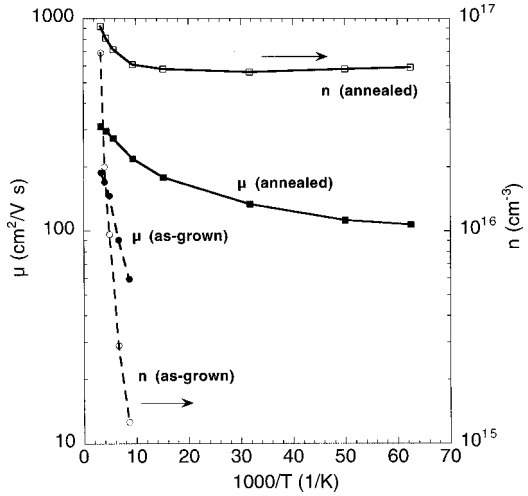

FIG. 2. Temperature dependence of Hall mobilities (solid symbol) and carrier concentrations (open symbol) for a MBE grown, *n*-type $In_{0.07}Ga_{0.93}As_{0.98}N_{0.02}$ sample as-grown (dashed line) and *ex situ* annealed (solid line) at 900 °C for 10 s.

Solar cells were constructed to evaluate the performance of MBE-grown devices and to determine minority carrier diffusion lengths. Our test-cells consisted of a thick (1 μm) InGaAsN base and a thin (0.1 μm), heavily doped [5×10^{17}/cm^3, Si(*n*) *or* Be(*p*)] InGaAsN emitter. There was a doped $Al_{0.3}Ga_{0.7}As$ window (400 Å thick) and a GaAs contact (300 Å thick) on top of the emitter. A series of *n*-on-*p* and *p*-on-*n* cells, annealed *in situ* at 620 °C for 30 min with an optional *ex situ* anneal at 900 °C for 10 s, were tested. Internal quantum efficiency (IQE) measurements for thick *p*-base (*n*-on-*p*, with and without *ex situ* anneal) and thick *n*-base (*p*-on-*n*, *ex situ* annealed) are shown in Fig. 3. Clearly, the thick *p*-base devices have higher IQEs indicating that the minority carrier, electron diffusion length is greater than that of the holes. With capacitance–voltage measurements of depletion layer widths and optical absorption data, minority carrier diffusion lengths were estimated from simulations of the measured IQE curves.[15] Calculated IQE curves are indicated by the dotted lines in Fig. 3. (Surface recombination was omitted from this simple model, producing a hump-like artifact above the GaAs band gap). Self-consistent fits of the cell IQEs were obtained with electron and hole diffusion lengths of 0.5 and 0.03 μm, respectively, in *ex situ* annealed MBE material and 0.25 and 0.03 μm in InGaAsN with only the *in situ* anneal. The higher temperature *ex situ* anneal produced a 2× increase in electron diffusion length.

Surprisingly, the diffusion lengths for annealed MBE material were reversed from those we reported for MOCVD-grown InGaAsN (0.01 μm for electrons and 0.9 μm for

holes).[6,11] Although we have presented evidence of point defects and inhomogeneities common to MBE and MOCVD materials, this variation of minority carrier properties indicates that there are yet other traps associated with each specific growth process. Overall, the IQEs and open circuit voltages of thick *p*-base MBE and thick *n*-base MOCVD solar cells were comparable. The air-mass-0, open circuit voltage of the annealed, thick *p*-base MBE cell in Fig. 3 was 0.43 V.

Our brief survey of the properties of MBE-grown InGaAsN (1.1 eV band gap) revealed many similarities to MOCVD material. Overall, the radiative efficiencies, Hall mobilities, device performance, and annealing behavior for MBE and MOCVD-grown InGaAsN were roughly comparable. We found evidence that annealing promotes the formation of In–N bonding like that reported for MOCVD material with lower nitrogen content. Annealed *n*-type, MBE-grown InGaAsN displayed a mobility temperature dependence which we had previously attributed to large-scale inhomogeneities. The maximum electron mobility was consistent with the limit imposed by alloy scattering, but there was no evidence of alloy-fluctuation-induced localization. However, some transport properties were unique to a particular growth process. MBE samples grown at lower temperature displayed a strongly thermally activated mobility and carrier concentration only prior to annealing, suggesting trap-modulated transport. In annealed MBE-grown solar cells electron diffusion was dominant (electron and hole diffusion lengths of 0.5 and 0.03 μm, respectively), whereas in MOCVD devices the minority carrier diffusion lengths were reversed with holes dominating. In summary, a comparison of MBE and MOCVD material revealed common, intrinsic point defects and inhomogeneities in InGaAsN, but minority carrier properties of InGaAsN remain unexplained by ''universal'' defect models.

The authors thank J. A. Bur and M. Bridges for technical support. Sandia is a multiprogram laboratory operated by Sandia Lockheed Martin Company, for the U.S. Department of Energy under Contract No. DE-AC04-94-AL85000.

[1] M. Weyers, M. Sato, and H. Ando, Jpn. J. Appl. Phys., Part 2 **31**, 853 (1992).
[2] W. G. Bi and C. W. Tu, Appl. Phys. Lett. **70**, 1608 (1997).
[3] M. Kondow, T. Kitatani, S. Nakatsuka, M. C. Larson, K. Nakahara, Y. Yazawa, and M. Okai, IEEE J. Sel. Top. Quantum Electron. **3**, 719 (1997).
[4] K. D. Choquette, J. F. Klem, A. J. Fischer, O. Blum, A. A. Allerman, I. J. Fritz, S. R. Kurtz, W. G. Breiland, R. M. Sieg, K. M. Geib, J. W. Scott, and R. L. Naone, Electron. Lett. **36**, 1388 (2000).
[5] S. R. Kurtz, D. Myers, and J. M. Olsen, *Proceedings of the 26th IEEE Photovoltaics Spec. Conference* (IEEE, New York, 1997), p. 875.
[6] S. R. Kurtz, A. A. Allerman, E. D. Jones, J. M. Gee, J. J. Banas, and B. E. Hammons, Appl. Phys. Lett. **74**, 729 (1999).
[7] E. V. K. Rao, A. Ougazzaden, Y. Le Bellego, and M. Juhel, Appl. Phys. Lett. **72**, 1409 (1998).
[8] V. Riede, H. Neumann, H. Sobotta, R. Schwabe, W. Siefert, and S. Schwetlick, Phys. Status Solidi A **93**, K151 (1986).
[9] S. Kurtz, J. Webb, L. Gedvilas, D. Friedman, J. Geisz, J. Olsen, R. King, D. Joslin, and N. Karam, Appl. Phys. Lett. **78**, 748 (2001).
[10] H. Ch. Alt, A. Yu. Egorov, H. Riechert, B. Wiedemann, J. D. Meyer, R. W. Michelmann, and K. Bethge, Physica B **302**, 282 (2001).
[11] S. R. Kurtz, A. A. Allerman, C. H. Seager, R. M. Sieg, and E. D. Jones, Appl. Phys. Lett. **77**, 400 (2000).
[12] C. Skierbiszewski, P. Perlin, P. Wisniewski, T. Suski, W. Walukiewicz, W. Shan, J. W. Ager, E. E. Haller, J. F. Geisz, D. J. Friedman, J. M. Olsen, and S. R. Kurtz, Phys. Status Solidi B **216**, 135 (1999).
[13] H. P. Xin, C. W. Tu, and M. Geva, Appl. Phys. Lett. **75**, 1416 (1999).
[14] S. G. Spruytte, C. W. Coldren, J. S. Harris, W. Wampler, P. Krispin, K. Ploog, and M. C. Larson, J. Appl. Phys. **89**, 4401 (2001).
[15] PCID Version 5.2, Copyright P. A. Basore and D. A. Clugston, University of New South Wales, Australia (1998).